

Highly Reactive Porphyrin–Iron–Oxo Derivatives Produced by Photolyses of Metastable Porphyrin–Iron(IV) Dipperchlorates

Zhengzheng Pan, Qin Wang, Xin Sheng, John H. Horner, and Martin Newcomb*

Department of Chemistry, University of Illinois at Chicago, 845 West Taylor Street, Chicago, Illinois 60607

Received October 4, 2008; E-mail: men@uic.edu

Abstract: Photolyses of metastable porphyrin–iron(IV) dipperchlorates in laser flash photolysis reactions gave highly reactive transients. The systems studied were 5,10,15,20-tetraphenylporphyrin (TPP), 5,10,15,20-tetramesitylporphyrin (TMP), and 2,3,7,8,12,13,17,18-octaethylporphyrin (OEP). The new species, which decayed within milliseconds in acetonitrile solutions, were shown to react with organic substrates by oxo-transfer reactions involving insertions into carbon–carbon double bonds of alkenes and styrenes or benzylic carbon–hydrogen bonds of arenes. The order of reactivity was OEP > TPP > TMP. Second-order rate constants for reactions with several substrates at 22 °C were determined; representative values of rate constants for the TPP derivative were $k = 8.6 \times 10^5 \text{ M}^{-1} \text{ s}^{-1}$ for styrene, $k = 2.5 \times 10^6 \text{ M}^{-1} \text{ s}^{-1}$ for cyclohexene, and $k = 7.7 \times 10^4 \text{ M}^{-1} \text{ s}^{-1}$ for ethylbenzene. These porphyrin–iron–oxo transients reacted 4–5 orders of magnitude faster than the corresponding iron(IV)–oxo porphyrin radical cations with rate constants similar to those of porphyrin–manganese(V)–oxo derivatives. Rate constants for oxidations of benzylic C–H positions of arenes correlated with the C–H bond dissociation energies, and Hammett correlations for reactions with substituted styrenes had ρ^+ values ranging from –0.5 to –0.7, reflecting electrophilic character of the oxidants and their high reactivity. On the basis of their unique UV–visible spectra, high reactivities, and oxo-transfer properties, the new transients are tentatively identified as porphyrin–iron(V)–oxo perchlorates, electronic isomers (or valence tautomers) of well-known iron(IV)–oxo porphyrin radical cations.

Introduction

Porphyrin–iron(III) complexes have been studied for decades as mimics for heme-containing peroxidase and cytochrome P450 enzymes^{1,2} and are important catalysts in laboratory and commercial oxidations.^{3–5} These complexes are oxidized to high-valent iron–oxo transients by sacrificial oxidants, and the iron–oxo species then oxidize substrates. Porphyrin–iron(IV)–oxo complexes are well characterized and relatively stable species, although their mechanisms of oxidation reactions apparently are complex.⁶ At the next higher level of oxidation, species with iron in a formal +5 oxidation state, the stable electronic isomers (or valence tautomers)⁷ are iron(IV)–oxo porphyrin radical cations, which are known in the biological context as Compounds I. Compounds I in enzymes were detected long ago, and iron(IV)–oxo porphyrin radical cation models of Compounds I have been known for decades.^{3–5}

Iron(IV)–oxo porphyrin radical cations are typically assumed to be the oxidizing transients in catalytic oxidations in the laboratory and in the cytochrome P450 enzymes. In kinetic studies, iron(IV)–oxo porphyrin radical cations appear to oxidize organic substrates in relatively uncomplicated two-electron, oxo-transfer reactions,⁸ but the rate constants for the oxidation reactions do not appear to be large enough to accommodate some catalytic results. For example, cyclohexane is oxidized with the porphyrin–iron species (TMP)Fe^{III}(Cl) as a catalyst and a sacrificial oxidant such as *m*-chloroperoxybenzoic acid (mCPBA),⁹ but iron(IV)–oxo porphyrin radical cations, (TMP)⁺Fe^{IV}(X), do not react appreciably with cyclohexane or other hydrocarbons at room temperature.⁸ In fact, (Porphyrin)⁺Fe^{IV}(X) species in general react relatively sluggishly in oxidations of benzylic C–H bonds,^{8,10,11} which have bond dissociation energies (BDEs) about 10 kcal/mol smaller than those for unactivated C–H bonds in hydrocarbons.¹² In a similar manner, Compound I of a cytochrome P450 enzyme

- (1) *Cytochrome P450 Structure, Mechanism, and Biochemistry*, 3rd ed.; Ortiz de Montellano, P. R., Ed.; Kluwer: New York, 2005.
- (2) Sono, M.; Roach, M. P.; Coulter, E. D.; Dawson, J. H. *Chem. Rev.* **1996**, *96*, 2841–2887.
- (3) Meunier, B. *Chem. Rev.* **1992**, *92*, 1411–1456.
- (4) Sheldon, R. A. *Metalloporphyrins in Catalytic Oxidations*; Marcel Dekker: New York, 1994.
- (5) *Metal-Oxo and Metal-Peroxo Species in Catalytic Oxidations*; Meunier, B., Ed.; Springer-Verlag: Berlin, 2000.
- (6) Pan, Z.; Newcomb, M. *Inorg. Chem.* **2007**, *46*, 6767–6774.
- (7) Weiss, R.; Bulach, V.; Gold, A.; Turner, J.; Trautwein, A. X. *J. Biol. Inorg. Chem.* **2001**, *6*, 831–845.

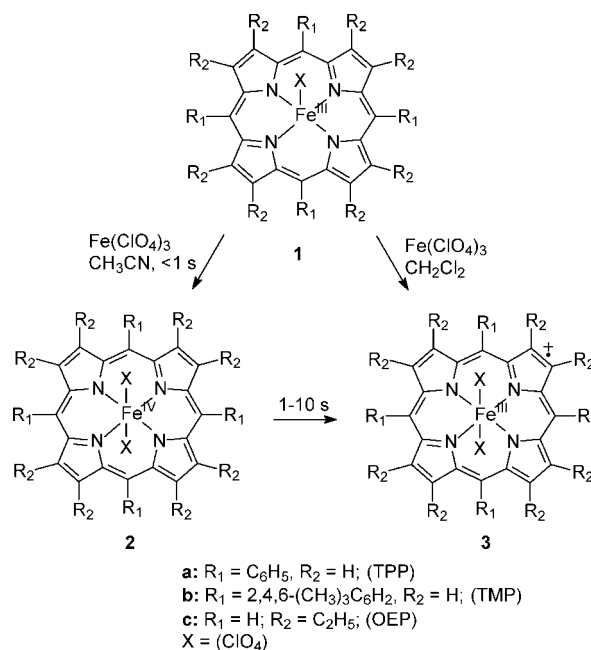
- (8) Pan, Z.; Zhang, R.; Newcomb, M. *J. Inorg. Biochem.* **2006**, *100*, 524–532.
- (9) Groves, J. T.; Haushalter, R. C.; Nakamura, M.; Nemo, T. E.; Evans, B. J. *J. Am. Chem. Soc.* **1981**, *103*, 2884–2886.
- (10) Zhang, R.; Chandrasena, R. E. P.; Martinez II, E.; Horner, J. H.; Newcomb, M. *Org. Lett.* **2005**, *7*, 1193–1195.
- (11) Zhang, R.; Nagraj, N.; Lansakara-P, D. S. P.; Hager, L. P.; Newcomb, M. *Org. Lett.* **2006**, *8*, 2731–2734.
- (12) Luo, Y.-R. *Handbook of Bond Dissociation Energies in Organic Compounds*; CRC Press: Boca Raton, FL, 2003.

reacted with a first-order rate constants for oxidation of unactivated C–H bonds of lauric acid substrate with $k_{\text{ox}} = 0.8 \text{ s}^{-1}$,^{13,14} whereas an estimated *minimum* value for the rate constant for oxidation of the unactivated C(5)-H bond in camphor by the reactive transient in cytochrome P450_{cam} is $k_{\text{ox}} > 1000 \text{ s}^{-1}$.^{15,16}

One possible explanation for the dichotomy between the observed relatively modest reactivities of Compounds **1** in enzymes and their models compared to the high reactivity required by oxidizing transients in some catalytic processes is that a more highly reactive (and undetected) species can be formed under catalytic conditions.¹⁷ If the “formal” iron(V) species initially produced in the catalytic sequence were indeed a “true iron(V)–oxo”¹⁸ species, these transients would be higher energy species and likely more reactive than their iron(IV)–oxo porphyrin radical cation isomers.^{18–20} Moreover, it is possible in principle that the high energy electronic isomers can be kinetically “trapped” such that they react in oxidation reactions in competition with relaxation to the more stable porphyrin radical cation isomer. In that regard, a recent study found considerable barriers for electronic isomerizations between iron(IV) neutral porphyrins and their iron(III) porphyrin radical cation isomers with $\Delta G^\ddagger = 19\text{--}21 \text{ kcal/mol}$.²¹

Limited numbers of iron(V)–oxo species employing “saturated” multidentate ligands have been reported,^{22,23} and no examples of true iron(V)–oxo species with aromatic porphyrin macrocyclic ligands are fully characterized. Nonetheless, our group developed a laser flash photolysis (LFP) photochemical method that produced highly reactive high-valent porphyrin– and corrole–iron–oxo species via oxy–ligand fragmentation reactions.^{24,25} The transients formed in these processes decay with lifetimes of only a few milliseconds, but they can be studied by UV–visible spectroscopy. They have been tentatively identified as iron(V)–oxo species on the basis of their unique UV–visible spectra, high reactivity, and demonstrated oxo-transfer chemistry in reactions with alkenes. In the present work, we report details of formation and kinetic studies of three high-

Scheme 1



valent porphyrin–iron–oxo derivatives formed by photolysis of porphyrin–iron(IV) diperchlorates.

Results and Discussion

The three systems studied in this work are shown in Scheme 1. 5,10,15,20-Tetraphenylporphyrin–iron(III) perchlorate, (TPP)– $\text{Fe}^{\text{III}}(\text{ClO}_4)$ (**1a**), 5,10,15,20-tetramesitylporphyrin–iron(III) perchlorate, (TMP) $\text{Fe}^{\text{III}}(\text{ClO}_4)$ (**1b**), and 2,3,7,8,12,13,17,18-octaethylporphyrin–iron(III) perchlorate, (OEP) $\text{Fe}^{\text{III}}(\text{ClO}_4)$ (**1c**), are known compounds. Oxidation of each complex **1** with ferric perchlorate was previously reported to give the corresponding iron(III) porphyrin radical cations (**3**).^{26–28} When the oxidation reactions were conducted in acetonitrile, however, metastable iron(IV) porphyrin diperchlorates **2** were initially formed,²¹ and these complexes then relaxed to the known complexes **3** within seconds.²¹

Figure 1A shows the kinetic behavior monitored at 396 nm upon mixing a solution of (TPP) $\text{Fe}^{\text{III}}(\text{ClO}_4)$ with a solution containing excess $\text{Fe}(\text{ClO}_4)_3$. The porphyrin–iron(IV) diperchlorate **2a** was formed in $\sim 0.3 \text{ s}$, and this transient converted to the iron(III) porphyrin radical cation diperchlorate **3a** with a half-life of ca. 10 s .²¹ The initial reaction forming **2a** is bimolecular, with a rate depending on the concentration of $\text{Fe}(\text{ClO}_4)_3$, but the decay of **2a** to **3a** is not. Thus, a large excess of $\text{Fe}(\text{ClO}_4)_3$ was not necessary to produce **2**, but a large concentration was required so that intermediates **2** formed fast enough to accumulate. At low concentrations with slow second-order reactions forming **2**, one would not necessarily detect intermediate **2**. In the original reports of oxidations of porphyrin–iron(III) complexes with ferric perchlorate,^{26–28} short-lived transients **2** were not detected, and we speculate that low concentrations of $\text{Fe}(\text{ClO}_4)_3$ resulted in long reaction times such that the iron(IV) transients **2** did not accumulate to

- (13) Newcomb, M.; Zhang, R.; Chandrasena, R. E. P.; Halgrimson, J. A.; Horner, J. H.; Makris, T. M.; Sligar, S. G. *J. Am. Chem. Soc.* **2006**, *128*, 4580–4581.
- (14) Sheng, X.; Horner, J. H.; Newcomb, M. *J. Am. Chem. Soc.* **2008**, *130*, 13310–13320.
- (15) Davydov, R.; Macdonald, I. D. G.; Makris, T. M.; Sligar, S. G.; Hoffman, B. M. *J. Am. Chem. Soc.* **1999**, *121*, 10654–10655.
- (16) Davydov, R.; Makris, T. M.; Kofman, V.; Werst, D. E.; Sligar, S. G.; Hoffman, B. M. *J. Am. Chem. Soc.* **2001**, *123*, 1403–1415.
- (17) Newcomb, M.; Chandrasena, R. E. P. *Biochem. Biophys. Res. Commun.* **2005**, *338*, 394–403.
- (18) Dey, A.; Ghosh, A. *J. Am. Chem. Soc.* **2002**, *124*, 3206–3207.
- (19) Ogliaro, F.; de Visser, S. P.; Groves, J. T.; Shaik, S. *Angew. Chem., Int. Ed.* **2001**, *40*, 2874–2878.
- (20) Koppenol, W. H. *J. Am. Chem. Soc.* **2007**, *129*, 9686–9690.
- (21) Pan, Z.; Harischandra, D. N.; Newcomb, M. *J. Inorg. Biochem.* **2009**, *103*, 174–181.
- (22) de Oliveira, F. T.; Chanda, A.; Banerjee, D.; Shan, X. P.; Mondal, S.; Que, L.; Bominaar, E. L.; Munck, E.; Collins, T. J. *Science* **2007**, *315*, 835–838.
- (23) Lee, S. H.; Han, J. H.; Kwak, H.; Lee, S. J.; Lee, E. Y.; Kim, H. J.; Lee, J. H.; Bae, C.; Lee, S. N.; Kim, Y.; Kimal, C. *Chem. Eur. J.* **2007**, *13*, 9393–9398.
- (24) Harischandra, D. N.; Zhang, R.; Newcomb, M. *J. Am. Chem. Soc.* **2005**, *127*, 13776–13777.
- (25) Pan, Z.; Zhang, R.; Fung, L. W. M.; Newcomb, M. *Inorg. Chem.* **2007**, *46*, 1517–1519.

- (26) Phillippi, M. A.; Goff, H. M. *J. Am. Chem. Soc.* **1982**, *104*, 6026–6034.
- (27) Groves, J. T.; Quinn, R.; McMurry, T. J.; Lang, G.; Boso, B. *J. Chem. Soc., Chem. Commun.* **1984**, 1455–1456.
- (28) Gans, P.; Buisson, G.; Duee, E.; Marchon, J. C.; Erler, B. S.; Scholz, W. F.; Reed, C. A. *J. Am. Chem. Soc.* **1986**, *108*, 1223–1234.

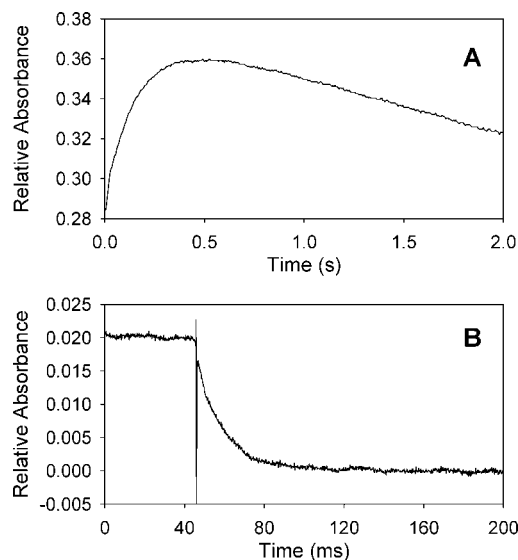


Figure 1. Kinetic traces. (A) Reaction of **1a** (2×10^{-5} M) with $\text{Fe}(\text{ClO}_4)_3$ (5×10^{-4} M) in acetonitrile at room temperature monitored at 396 nm; the iron(IV) complex **2a** was formed in 0.3 s and decayed to **3a**. (B) Laser irradiation of **2b** monitored at 403 nm; the pretrigger sequence was initiated ($t = 0$ ms) at 0.2 s after mixing, and the laser fired ca. 50 ms later.

detectable levels.²¹ Although an excess of $\text{Fe}(\text{ClO}_4)_3$ was necessary to give a fast bimolecular reaction when the concentrations of **1** were small, as in our kinetic studies using UV–vis detection, we describe a product experiment below where the concentration of **1** was greater, and an excess of $\text{Fe}(\text{ClO}_4)_3$ was not required. Similarly, samples of **2** prepared for NMR and EPR studies did not contain large excesses of $\text{Fe}(\text{ClO}_4)_3$.²¹

In order to permit kinetic studies of the transients formed by photolyses of intermediates **2**, the oxidation reactions of **1** were performed in a stopped-flow mixing cell that was mounted in a LFP kinetic unit. Solutions of complexes **1** and $\text{Fe}(\text{ClO}_4)_3$ in CH_3CN were rapidly mixed, and the resulting mixtures were irradiated with 355 nm laser light after short delays to permit complete formation of complexes **2**. Figure 1B shows typical kinetic behavior when **1b** was oxidized with $\text{Fe}(\text{ClO}_4)_3$ to give complex **2b**, which was then irradiated with 355 nm laser light. The laser pulse at $t \approx 50$ ms resulted in a small amount of “instant” bleaching due to formation of the new species in the photochemical reaction, and the newly formed species rapidly decayed in the subsequent 50 ms. Importantly, irradiation of iron(III) porphyrin radical cation complexes **3** with 355 nm laser light under the same conditions as used for irradiation of species **2** resulted in *no noticeable reactions*.

Kinetic behavior similar to that shown in Figure 1 was found for each of the three systems studied in this work. Photolysis of solutions containing the iron(IV) complexes **2** with 355 nm light gave new transients **4** that decayed rapidly at room temperature. Time-resolved decay spectra for these new transients were constructed by monitoring the decay with monochromatic light at varying intervals. Figure 2 shows the results for each system. In these representations, positive peaks are from signals decaying with time, and negative peaks are from signals forming with time. Thus, the spectra in Figure 2 show the differences in absorbances between the photochemically generated transient and the product of its reactions. It is possible in principle to reconstruct the spectrum of the initially formed transient by adding a spectrum of the “final” product to the spectra in Figure 2, but as with many porphyrin iron complexes, the Soret bands of various complexes have similar absorbances.

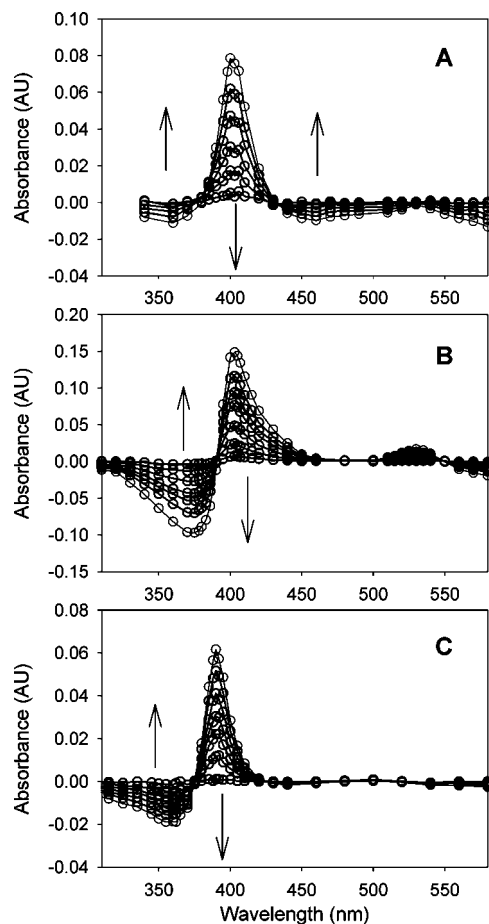


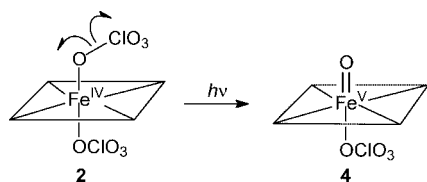
Figure 2. Time-resolved UV–visible spectra for reactions in CH_3CN at room temperature for (A) TPP complex **4a** reacting over 100 ms, (B) TMP complex **4b** reacting over 100 ms, and (C) OEP complex **4c** reacting over 30 ms.

For example, the λ_{max} values for **2a**, **2b**, and **2c** in CH_3CN are 396, 397, and 391 nm, respectively,²¹ which are similar to the apparent λ_{max} values for the new transients shown in Figure 2. Accordingly, spectra of transients **4** constructed by adding spectra of complexes **2** to the experimental results would give new spectra with Soret band and signals quite similar to those apparent in the time-resolved spectra in Figure 2.

From the spectra, the kinetic behavior that is discussed below, and the oxo-transfer properties of the intermediates described later, one can deduce that the new transients are high energy iron–oxo species of some type formed by photochemically activated O–Cl bond cleavages of a perchlorate ligand. The high reactivity of these transients, i.e., millisecond lifetimes at room temperature, precluded their characterizations by various classical methods, but both the UV–visible spectra and the reactivities exclude known iron–oxo species. For example, TMP–iron derivatives are especially well studied, and we prepared samples of TMP–iron derivatives for comparison of the UV–visible spectra and kinetic behavior in acetonitrile. For the porphyrin–iron(IV)–oxo species $(\text{TMP})\text{Fe}^{\text{IV}}(\text{O})$ ^{6,29} and the iron(IV)–oxo porphyrin radical cations $(\text{TMP})^+\text{Fe}^{\text{IV}}(\text{O})(\text{X})$ where $\text{X} = \text{Cl}$ or ClO_4 ,^{8,9} the UV–visible spectra differed from that of **4b**, especially in the changes observed upon reaction. The Compound I analogues have broad Soret bands, and the

(29) Groves, J. T.; Gross, Z.; Stern, M. K. *Inorg. Chem.* **1994**, *33*, 5065–5072.

Scheme 2



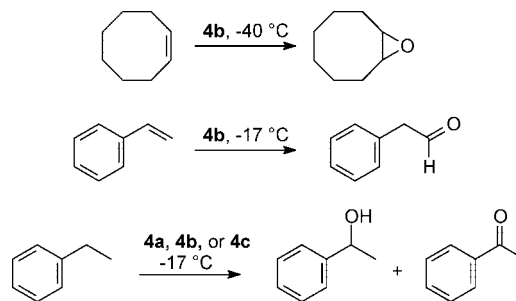
absorbances in the range 350–450 nm increase when these complexes react to give iron(III) products,⁸ whereas the absorbance between 390 and 450 nm decreases upon reaction of **4b**. In addition, Compound I analogs are orders of magnitude less reactive than **4b** both in self-decay reactions (presumably reactions with solvent) and in reactions with organic substrates.⁸

One can logically exclude simple excited states of species **2** or iron–oxo derivatives for the identities of transients **4** because millisecond lifetimes are too long for excited states of open shell porphyrin–metal species, which more typically relax with subnanosecond lifetimes.³⁰ Nonetheless, another formal excited-state seems to be a reasonable candidate for species **4**. Specifically, homolytic cleavages of O–Cl bonds in the perchlorate ligands could give porphyrin–iron(V)–oxo species, which are electronic isomers (or valence tautomers)⁷ of iron(IV)–oxo porphyrin radical cations (Scheme 2), and we tentatively assign complexes **4** as such iron(V)–oxo species. If the new transients indeed are iron(V)–oxo species, they would be isolated kinetically from their more stable isomers by barriers for internal redox reactions, and it is noteworthy in that regard that substantial kinetic barriers isolate the porphyrin–iron(IV) diperchlorates **2** from their thermodynamically favored iron(III) porphyrin radical cations **3**; the measured barriers for conversions of **2** to **3** were $\Delta G^\ddagger \approx 20$ kcal/mol.²¹

The photochemically activated cleavage reaction shown in Scheme 2 is related to other photochemically activated ligand cleavage reactions that are known to give high-valent metal–oxo complexes. Porphyrin–manganese(III) complexes and corrole–manganese(IV) complexes containing oxygen-bound ligands such as perchlorate were cleaved by 355 nm laser light to give high-valent manganese–oxo species,^{30–33} and corrole–iron(IV) nitrate and chlorate complexes were cleaved photochemically to give a transient tentatively identified as a corrole–iron(V)–oxo species.²⁴ In analogous reactions, iron(V)–nitrido complexes also can be prepared by photochemically induced ligand fragmentation reactions.^{34–37} Furthermore, an iron(VI)–nitrido complex was prepared in a photochemically driven ligand cleavage reaction,³⁸ and we cannot exclude formal iron(VI)–oxo complexes, produced by heterolytic cleavage of the perchlorate ligand O–Cl bond, as possible structures for **4**.

Transients **4** were shown to react as oxo-transfer agents in “bulk” reactions with cyclooctene, styrene, and ethylbenzene.

Scheme 3



In these studies, the metastable diperchlorates **2** were prepared at low temperatures where they had multisecond to multimicrosecond lifetimes.²¹ Organic substrates were present to the reaction mixtures, and the mixtures were irradiated with >300 nm light. Scheme 3 summarizes the results of the bulk reactions with organic substrates.

When precursor **2b** was prepared in acetonitrile at -40 °C from reaction of **1b** with 1.2 equiv of $\text{Fe}(\text{ClO}_4)_3$, the estimated yields of **2b** determined from UV–visible spectroscopy was 80%, and complex **2b** was stable for minutes at -40 °C.²¹ A solution containing **2b** was thus prepared in the presence of an excess of cyclooctene, and the mixture was irradiated in a light box with 300–400 nm light. GC analysis of the product mixture showed that cyclooctene oxide was formed in 28% yield based on the porphyrin diperchlorate species **2b** or 22% based on **1b** initially employed. Control reactions showed that no epoxide product was formed when **1b**, $\text{Fe}(\text{ClO}_4)_3$, or the light was omitted.

In a somewhat different bulk experiment, precursor **2b** was prepared in 2 mL of CH_3CN at -17 °C from a dilute solution of **1b** (ca. 2×10^{-5} M) in the presence of 25 equiv of $\text{Fe}(\text{ClO}_4)_3$. Excess styrene (100 equiv based on porphyrin) was added, and the mixture was irradiated with 20 10-J pulses of 320–490 nm light delivered in 0.5 s each. The major product formed was phenylacetaldehyde, identified by GC and GC–mass spectral analysis and obtained in about 50% yield based on the initial porphyrin–iron complex. A series of control reactions demonstrated that no oxidation product was formed when the porphyrin–iron complex, the ferric perchlorate, or the light was omitted. Another important control reaction showed that styrene oxide was quantitatively converted to phenylacetaldehyde under the reaction condition but with no irradiation. Thus, **4b** reacted by oxygen transfer to styrene, and we assume that styrene oxide was formed in the initial oxidation reaction and subsequently isomerized to phenylacetaldehyde.

A series of product studies similar to the experiment described above was conducted with excess ethylbenzene present. Precursors **2** were prepared in acetonitrile at -17 °C and irradiated in the presence of ethylbenzene. The products found in these reactions, as determined by GC and GC–mass spectrometry analyses, were 1-phenylethanol and acetophenone. Control reactions demonstrated that no oxidation product was formed when the porphyrin–iron complexes, the ferric perchlorate, or the light was omitted from the reaction, nor was any oxidation product formed when transients **2** were allowed to decay to **3** before the photolyses. Furthermore, 1-phenylethanol was shown to be stable to the reaction conditions in the absence of light, indicating that acetophenone was formed by successive oxidations of ethylbenzene to 1-phenylethanol and then 1-phenylethanol to acetophenone, both by photochemically generated

- (30) Zhang, R.; Horner, J. H.; Newcomb, M. *J. Am. Chem. Soc.* **2005**, *127*, 6573–6582.
 (31) Zhang, R.; Newcomb, M. *J. Am. Chem. Soc.* **2003**, *125*, 12418–12419.
 (32) Zhang, R.; Harischandra, D. N.; Newcomb, M. *Chem. Eur. J.* **2005**, *11*, 5713–5720.
 (33) Zhang, R.; Newcomb, M. *Acc. Chem. Res.* **2008**, *41*, 468–477.
 (34) Wagner, W. D.; Nakamoto, K. *J. Am. Chem. Soc.* **1988**, *110*, 4044–4045.
 (35) Wagner, W. D.; Nakamoto, K. *J. Am. Chem. Soc.* **1989**, *111*, 1590–1598.
 (36) Meyer, K.; Bill, E.; Mienert, B.; Weyhermuller, T.; Wieghardt, K. *J. Am. Chem. Soc.* **1999**, *121*, 4859–4876.
 (37) Aliaga-Alcalde, M.; George, S. D.; Mienert, B.; Bill, E.; Wieghardt, K.; Neese, F. *Angew. Chem., Int. Ed.* **2005**, *44*, 2908–2912.
 (38) Berry, J. F.; Bill, E.; Bothe, E.; George, S. D.; Mienert, B.; Neese, F.; Wieghardt, K. *Science* **2006**, *312*, 1937–1941.

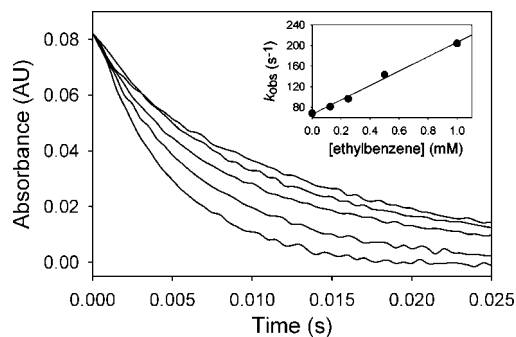


Figure 3. Kinetic traces at 403 nm for reactions of (TMP) derivative **4b** at 22 °C in acetonitrile with ethylbenzene at (from the top) 0.0, 0.13, 0.25, 0.50, and 1.0 mM concentrations. The inset shows a plot of the pseudo-first-order rate constants versus the concentration of ethylbenzene.

species. The yields of oxidation products in the ethylbenzene reactions were 90% (**1a**), 80% (**1b**), and 40% (**1c**) based on porphyrin–iron complex if we assume that 2 equiv of oxidant were consumed in formation of acetophenone.

It is noteworthy that, although a porphyrin–iron complex can turn over multiple times in the bulk photolysis reactions in principle, turnover will be limited. We estimate from the observed kinetics that the reactions of species **4** with ethylbenzene would be about one to three times as fast as competing decay in the background reaction, presumably by reaction with solvent, but another process that limits turnover is conversion of the porphyrin–iron(IV) diperchlorate complexes **2** to dead-end species **3**, which competes with the photoactivated ligand fragmentation reactions of **2**. Indeed, UV–visible spectroscopic analysis of the product mixtures after the bulk photolyses indicated the presence of iron(III) porphyrin radical cations **3**.

Kinetic studies for reactions of transients **4** with organic substrates were performed by generating **4** in LFP studies in acetonitrile in the presence of varying (high) concentrations of organic reductants. Kinetics could be measured at various wavelengths, but we typically followed changes in absorbance in the Soret band region. Intermediates **4** decayed rapidly in CH₃CN, and the rates were greatly accelerated when organic reductants were present. Figure 3 shows a typical set of results for reaction of **4b** with ethylbenzene. All reactions were performed under pseudo-first-order conditions, and each kinetic trace was well approximated by a single exponential decay or growth function. For reactions run under pseudo-first-order conditions, the second-order rate constant is given by eq 1, where k_{obs} is the observed pseudo-first-order rate constant, k_0 is a background rate constant, k_{ox} is the second-order rate constant, and [Subs] is the concentration of substrate. The inset in Figure 3 shows the kinetic data plotted according to eq 1.

$$k_{\text{obs}} = k_0 + k_{\text{ox}}[\text{Subs}] \quad (1)$$

Kinetic studies were performed with alkene substrates, including substituted styrenes, and arene substrates containing reactive benzylic C–H bonds. Pseudo-first-order rate constants (k_{obs}) were determined with varying concentrations of substrate, and the data were analyzed via eq 1 using a linear regression fit with weighting to obtain the second-order rate constants for oxidation (k_{ox}). The kinetic measurements for the TPP–iron complex **4a** were typical, and the results for **4a** are shown in Figure 4. Table 1 contains the kinetic results. For the series of oxidants studied in this work, the octaethylporphyrin species was the most reactive species, and the tetraphenylporphyrin species was slightly more reactive than the tetramesitylporphyrin species.

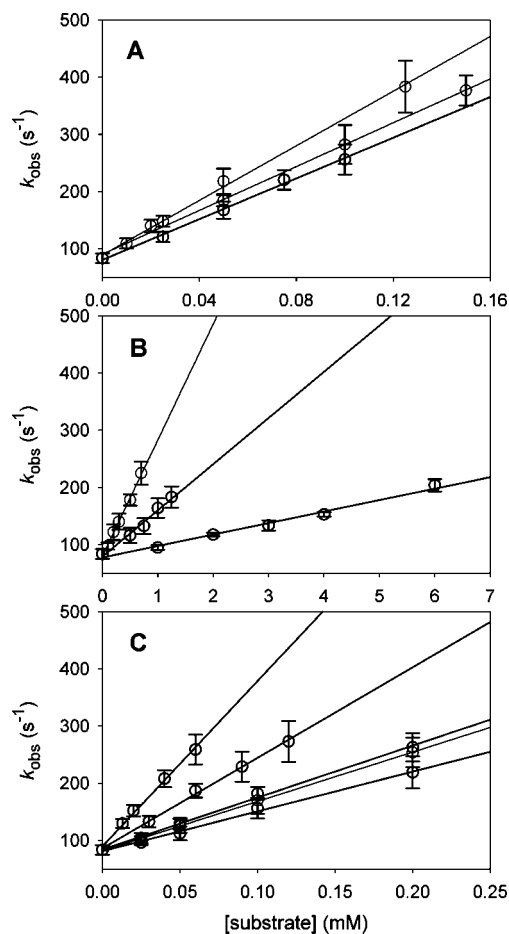


Figure 4. Kinetic results for reactions of **4a** (A) with alkenes (from the top: cyclohexane, *trans*-stilbene, cyclooctene), (B) with arenes (from the top: diphenylmethane, ethylbenzene, ethylbenzene-*d*₁₀), and (C) with styrenes (from the top: *p*-methoxystyrene, *p*-methylstyrene, *p*-fluorostyrene, styrene, *p*-chlorostyrene).

It is important to note that, under our experimental conditions, secondary oxidations of substrates were not important in the kinetics. The concentration of precursors **2** employed in the kinetic studies was ca. 1×10^{-5} M, and the conversion of **2** to **4** in the LFP had estimated efficiencies of ca. 10% as judged by the extent of signal change in the Soret band region observed in the decay reactions shown in Figure 2. Thus, the primary oxidation products were formed at concentrations smaller than 1×10^{-6} M, and their average concentrations during the reactions were submicromolar. In the case of oxidations of alkenes and styrenes, the rate constants for oxidations of the epoxide products are expected to be *smaller* than those for oxidations of the alkenes and styrenes from consideration of the kinetics of iron(IV)–oxo porphyrin radical cations.⁸ In the case of oxidations of arenes, the secondary oxidation reactions might be faster than the initial oxidations the arenes, but the concentrations of arenes in the pseudo-first-order kinetic studies were 5–8 orders of magnitude greater than those of the first-formed oxidation products. Accordingly, secondary oxidations were expected to be much less than 1% of the total reactions in all kinetic studies.

The most striking kinetic results are the tremendously large rate constants for reactions of derivatives **4** in comparison to those for other iron–oxo derivatives. This is illustrated in Table 2, which lists rate constants for oxidations of cyclooctene and ethylbenzene by **4b** and by the macrocyclic ligand–metal–oxo

Table 1. Rate Constants for Reactions of Porphyrin–Iron–Oxo Complexes **4** with Organic Reductants^a

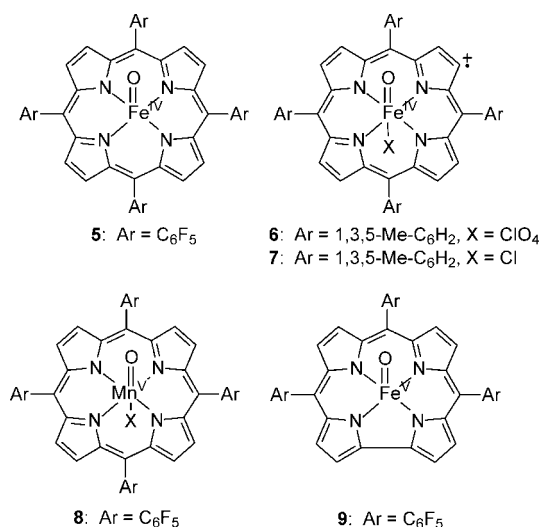
substrate	(TPP)Fe ^V (O)(ClO ₄) (4a)	(TMP)Fe ^V (O)(ClO ₄) (4b)	(OEP)Fe ^V (O)(ClO ₄) (4c)
none ^b	77 s ⁻¹	84 s ⁻¹	134 s ⁻¹
<i>cis</i> -stilbene	nd ^c	(2.0 ± 0.1) × 10 ⁶	nd
<i>trans</i> -stilbene	(2.0 ± 0.2) × 10 ⁶	(1.7 ± 0.1) × 10 ⁶	(7.2 ± 0.5) × 10 ⁶
cyclohexene	(2.5 ± 0.3) × 10 ⁶	(2.2 ± 0.1) × 10 ⁶	(1.02 ± 0.11) × 10 ⁷
<i>cis</i> -cyclooctene	(1.8 ± 0.2) × 10 ⁶	(1.6 ± 0.2) × 10 ⁶	(6.3 ± 0.4) × 10 ⁶
triphenylmethane	nd	(2.5 ± 0.2) × 10 ⁵	nd
diphenylmethane	(2.0 ± 0.2) × 10 ⁵	(1.5 ± 0.2) × 10 ⁵	(3.9 ± 0.5) × 10 ⁵
cumene	nd	(7.1 ± 0.8) × 10 ⁴	nd
ethylbenzene	(7.7 ± 1.3) × 10 ⁴	(1.4 ± 0.2) × 10 ⁵	(2.9 ± 0.3) × 10 ⁵
ethylbenzene- <i>d</i> ₁₀	(1.94 ± 0.14) × 10 ⁴	(1.1 ± 0.3) × 10 ⁴	nd
toluene	nd	(5.6 ± 0.7) × 10 ⁴	nd
styrene	(8.6 ± 1.2) × 10 ⁵	(7.5 ± 0.8) × 10 ⁵	(3.6 ± 0.4) × 10 ⁶
4-chlorostyrene	(6.9 ± 1.2) × 10 ⁵	(6.2 ± 0.7) × 10 ⁵	(3.4 ± 0.3) × 10 ⁶
4-fluorostyrene	(9.5 ± 1.0) × 10 ⁵	(8.2 ± 0.6) × 10 ⁵	(4.0 ± 0.4) × 10 ⁶
4-methylstyrene	(1.65 ± 0.18) × 10 ⁶	(1.22 ± 0.13) × 10 ⁶	(6.7 ± 0.4) × 10 ⁶
4-methoxystyrene	(3.0 ± 0.3) × 10 ⁶	(2.74 ± 0.18) × 10 ⁶	(9.2 ± 0.6) × 10 ⁶

^a Second-order rate constants in units of M⁻¹ s⁻¹ unless noted for reactions in acetonitrile at 22 ± 1 °C; errors are 1σ. ^b Rate constants with no substrate are pseudo-first-order rate constants for decay in acetonitrile. ^c nd = not determined.

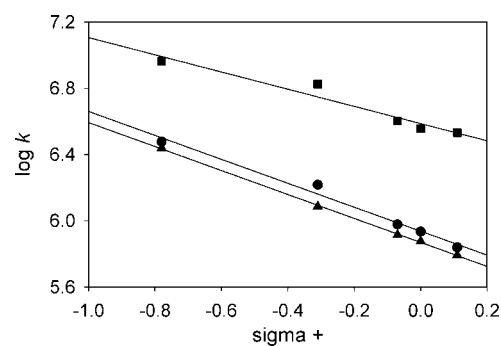
Table 2. Rate Constants for Oxidations of Cyclooctene and Ethylbenzene by Macrocyclic Ligand–Metal–Oxo Complexes^a

porphyrin–metal–oxo ^b	cyclooctene	ethylbenzene	ref
(TPFPP)Fe ^{IV} O (5)	< 1.8 × 10 ⁻²		6
(TMP) ⁺ Fe ^{IV} (O)(ClO ₄) (6)	6.2 × 10	1.3	8
(TMP) ⁺ Fe ^{IV} (O)(Cl) (7)	2.9 × 10 ²	4.5	8
(TPFPP)Mn ^V (O)(X) (8)	6 × 10 ⁵ ^c	1.3 × 10 ⁵	30
(TPFPC)Fe ^V (O) (9)	5.9 × 10 ³	5.7 × 10 ²	24
(TMP)Fe ^V (O)(ClO ₄) (4b)	1.6 × 10 ⁶	1.4 × 10 ⁵	this work

^a Second-order rate constants in units of M⁻¹ s⁻¹ for reactions at 22 °C. ^b (TPFPP) = 5,10,15-*tetrakis*(pentafluorophenyl)porphyrin; (TMP) = 5,10,15,20-*tetramesityl*porphyrin; (TPFPC) = 5,10,15-*tris*(pentafluorophenyl)corrole. ^c Rate constant for reaction with *cis*-stilbene.

Chart 1

complexes shown in Chart 1. Complex **5** is a neutral porphyrin iron(IV)–oxo species which likely reacts via initial disproportionation to give a more reactive iron(IV)–oxo porphyrin radical cation that effects oxidation reactions;⁶ therefore, the rate constant in Table 2 for **5** is a maximum value. Complexes **6** and **7** are iron(IV)–oxo porphyrin radical cations, and **6** is an isomer of **4b**. The rate constants for reactions of the (TMP) Compound I analogues **6** and **7** are several orders of magnitude smaller than those for complex **4b**.⁸ Complex **8** is a highly reactive manganese(V)–oxo species where the counterion X is most likely perchlorate,³⁰ and we note that the aryl groups on

**Figure 5.** Hammett plots for reactions of styrenes with (TPP) derivative **4a** (●), (TMP) derivative **4b** (▲), and (OEP) derivative **4c** (■) in acetonitrile at 22 °C.

the porphyrin in complex **8** are electron-withdrawing pentafluorophenyl groups that activate this oxidant in comparison to a tetraphenylporphyrin.³⁰ The putative (TMP)–iron(V)–oxo species **4b**, is about 5 orders of magnitude more reactive than isomer **6**, and similar in reactivity to the activated manganese(V)–oxo species **8**.

The high reactivity of iron–oxo transients **4** and their tentative identification as iron(V)–oxo species is consistent with the reactivity of another possible iron(V)–oxo derivative. The putative 5,10,15-*tris*(pentafluorophenyl)corrole–iron(V)–oxo derivative, (TPFPC)Fe^V(O) (**9**), was produced in a photochemical cleavage reaction similar to the photolyses of iron(IV) diperchlorates **2**.²⁴ The iron–oxo derivatives **4** produced in this work are 2–3 orders of magnitude more reactive than species **9** in epoxidation of cyclooctene and hydroxylation of ethylbenzene. Corroles are trianionic macrocyclic ligands as opposed to dianionic porphyrins, and high-valent metal–oxo corrole derivatives are well known to be more stable than their porphyrin analogues.³⁹ Therefore, derivatives **4** would be expected to be more reactive than **9** if both types of transients contain iron(V)–oxo moieties.

The series of substituted styrenes was studied to permit Hammett analyses of the electron demand in the oxidation reactions. Figure 5 shows Hammett plots where we used the σ^+ substituent values. For both the (TPP) and (TMP) derivatives **4a** and **4b**, the plots have slopes of $\rho^+ = -0.72$, and the (OEP)

(39) Gross, Z.; Gray, H. B. *Comment. Inorg. Chem.* **2006**, *27*, 61–72.

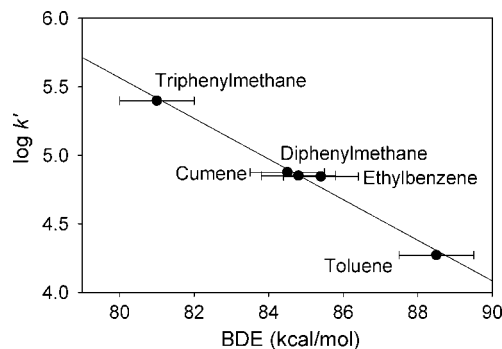


Figure 6. Correlation between statistically corrected second-order rate constants for reactions of benzylic C–H bonds with (TMP) derivative **4b** with the homolytic BDEs.

derivative **4c** has $\rho^+ = -0.52$. The negative values of the slopes indicate that the transition states for the reactions involve development of positive charge on the styrene α -carbons as expected for oxo transfer reactions from electrophilic reactants, and the relatively small values of the slopes reflect the high reactivity of the iron–oxo derivatives and corresponding early transition states. For the same series of styrenes as studied in this work, the Compound I analogues $(\text{TMP})^+\text{Fe}^{\text{IV}}(\text{O})(\text{ClO}_4)$ (**6**) and $(\text{TMP})^+\text{Fe}^{\text{IV}}(\text{O})(\text{Cl})$ (**7**) reacted with ρ^+ values of -1.96 and -0.89 , respectively.⁸ The difference in the Hammett reaction parameters for the isomers $(\text{TMP})^+\text{Fe}^{\text{IV}}(\text{O})(\text{ClO}_4)$ (**6**, $\rho^+ = -1.96$) and $(\text{TMP})\text{Fe}^{\text{V}}(\text{O})(\text{ClO}_4)$ (**4b**, $\rho^+ = -0.72$) is a direct reflection of differences in the extent of charge development in the transition states, which is likely due primarily to the relative positions of the transition states on the reaction coordinates, with the more reactive species having an earlier transition state.

For the (TMP) derivative **4b**, we measured rate constants for reactions of a series of aromatic compounds with benzylic C–H bonds with decreasing BDEs, toluene, ethylbenzene, cumene, diphenylmethane, and triphenylmethane. All free energy relationships predict that the rate constants for C–H functionalization reactions will have an exponential relationship to the free energy change of the reactions as long as the nature of reactions changes only slightly from one substrate to the next. Consistent with these predictions, a plot of the log of the statistically corrected first-order rate constants versus the BDEs of the benzylic C–H bonds¹² gives an excellent line (Figure 6). The small absolute value for the slope of the line (-0.15) indicates early transition states for the reactions reflecting the high reactivity of the transient iron–oxo species.

We noted in the Introduction that it is commonly assumed that the active oxidants formed from porphyrin–iron(III) catalysts and sacrificial oxidants are iron(IV)–oxo porphyrin radical cations. Paradoxically, kinetic studies suggest that iron(IV)–oxo porphyrin radical cations might not be active enough to be the true oxidants under catalytic turnover conditions.⁸ For example, $(\text{TMP})\text{Fe}(\text{Cl})$ as a catalyst with iodosylbenzene⁴⁰ or sodium hypochlorite⁴¹ as sacrificial oxidants will hydroxylate unactivated C–H bonds in hydrocarbons, but the $(\text{TMP})^+\text{Fe}^{\text{IV}}(\text{O})(\text{X})$ Compound I models **6** and **7** reacted sluggishly in single-turnover kinetic studies.⁸ One method to characterize the transients in the oxidation processes is to measure relative rate constants for oxidations in competition

Table 3. Ratios of Rate Constants for Reactions of Pairs of Substrates^a

substrates (A/B) ^b	k_A/k_B (PhIO) ^c	k_A/k_B (4b) ^d	k_A/k_B (6) ^e
<i>cis</i> -stilbene/diphenylmethane	24	13	69
<i>cis</i> -stilbene/ethylbenzene	18 ^f	14	56
cyclooctene/ <i>trans</i> -stilbene	3.7	0.9	18
<i>cis</i> -stilbene/cyclohexene	0.8	0.9	1.3
<i>cis</i> -stilbene/cyclooctene	1.2	1.2	1.5
ethylbenzene/diphenylmethane	1.0	0.9	1.2
ethylbenzene/ethylbenzene- <i>d</i> ₁₀		13	55 ^g
styrene/diphenylmethane		5	15

^a For reactions in acetonitrile at 22 ± 2 °C. ^b Substrate A is listed first. ^c Ratio of rate constants determined from competition reactions employing **1b** and PhIO unless noted; data from ref 8. ^d Ratio of rate constants for **4b** determined in this work. ^e Data from ref 8 unless noted. ^f The sacrificial oxidant was *m*-chloroperoxybenzoic acid. ^g Data from ref 42.

reactions under catalytic conditions and compare these values to the ratios of rate constants for reactions of the isolated oxidants. Such a comparison is shown in Table 3. Ratios of absolute rate constants for reactions of two substrates with the (TMP) oxidant **4b** are from this work, and ratios of absolute rate constants for reactions of the same substrates with $(\text{TMP})^+\text{Fe}^{\text{IV}}(\text{O})(\text{ClO}_4)$ (**6**) were previously reported as were the ratios of rate constants from competitive reactions where mixtures of the two substrates reacted with $(\text{TMP})\text{Fe}^{\text{III}}(\text{ClO}_4)$ and a sacrificial oxidant.⁸

The ratios of rate constants for reactions of **4b** and **6** clearly reflect the large difference in reactivity of these isomers, with the more reactive species **4b** displaying reduced selectivity in comparison to **6** for any pair of substrates. In comparison to the results of the competition experiments under turnover conditions, the ratios of rate constants for the Compound I analogue **6** are consistently larger than the ratios found for the catalytic turnover reactions. The ratios for reactions of iron–oxo transient **4b** are smaller than the ratios from the competition reactions in half of the cases and the same as the competition ratio in the other half. These results suggest that the highly reactive species **4b** is a major species involved in the oxidation reactions under turnover conditions where the active transient is not detected.

Another pair of rate constants in Table 3 is noteworthy. For oxidations of ethylbenzene and ethylbenzene-*d*₁₀ by the (TMP) derivative **4b**, the kinetic isotope effect of $k_{\text{H}}/k_{\text{D}} = 13$ is large enough to suggest that there is a tunneling component in this reaction. Further study is required to address that possibility, but we note that the compounds **6** and **7**, which are iron(IV)–oxo porphyrin radical cation analogues of **4b**, display much larger tunneling components in similar oxidations.⁴² Large tunneling contributions also were found in hydrocarbon oxidations catalyzed by $(\text{TMP})\text{Fe}^{\text{III}}\text{Cl}$.⁴¹

Conclusion

Photolyses of metastable porphyrin–iron(IV) diperchlorates produced previously unknown and highly reactive iron–oxo transients. Methods for productions of these species under conditions where they are long-lived are desired so that more complete characterizations are possible, but the unique UV–visible spectral properties, oxo-transfer properties, and kinetic values of these new species suggest a tentative identification as porphyrin–iron(V)–oxo complexes. These iron–oxo species

(40) Groves, J. T.; Nemo, T. E. *J. Am. Chem. Soc.* **1983**, *105*, 6243–6248.

(41) Sorokin, A. B.; Khenkin, A. M. *J. Chem. Soc. Chem. Commun.* **1990**, 45–46.

(42) Pan, Z.; Horner, J. H.; Newcomb, M. *J. Am. Chem. Soc.* **2008**, *130*, 7776–7777.

oxidize alkenes, styrenes and arenes with benzylic C–H bonds in two-electron, oxo-transfer reactions that are several orders of magnitude faster than oxidations by iron(IV)–oxo porphyrin radical cations. As deduced from ratios of rate constants for oxidation reactions, it is possible that these newly found transients are involved in part in oxidations catalyzed by porphyrin–iron(III) complexes.

Experimental Section

Materials. The porphyrin–iron(IV) diperchlorate complexes **2** in acetonitrile solutions were prepared as previously reported²¹ using Biotech grade acetonitrile (>99.93% anhydrous) (Sigma-Aldrich). Mixing experiments, including LFP experiments, were conducted on an Applied Photophysics LKS-60 kinetic spectrometer equipped with an SC-18MV stopped-flow mixing unit.

Kinetic Studies. The methods were similar to those employed in LFP studies of radical reactions.^{43,44} Kinetic studies were conducted at 21 ± 2 °C, and oversampling (64:1) was employed to improve the signal-to-noise ratio. In a typical reaction, 100 μL of a CH_3CN solution of $\text{Fe}(\text{ClO}_4)_3$ (2.5×10^{-4} M) was mixed in a 2 mm \times 10 mm optical cell with an equal volume (100 μL) of porphyrin–iron(III) perchlorate species **1** (2.0×10^{-5} M) in CH_3CN . For kinetic studies with substrates, the substrate at the desired concentration was present in the solution containing complex **1**. After a delay of 0.5–1 s to permit formation of porphyrin–iron(IV) diperchlorate species **2**, the solution was irradiated with a 355 nm light from a Nd:YAG laser (ca. 7 ns pulse, ca. 10 mJ). The reactions were monitored at single wavelengths on photomultiplier tubes with 2 ns rise times. Data were acquired and analyzed with the Applied

Photophysics software to give pseudo-first-order rate constants with five or six different concentrations of substrate. Second-order rate constants were determined from these data with a weighted linear least-squares analysis; errors in the second-order rate constants are at 1σ .

Products from Bulk Photolysis Reactions. The apparatus was a temperature-regulated chamber that held a 10 mm \times 10 mm UV–visible spectroscopy cell. Fiber optics cables were mounted in the chamber, and UV–visible spectra were monitored by an Ocean Optics USB4000 miniature fiber optic spectrometer. Light from an EXOS Novacure N2001-A spot photolysis unit (10 J of 320–500 nm light per 0.5 s pulse) was delivered into the chamber via a gel optical cable. In a typical reaction, a solution of **1b** (1.56×10^{-5} M) and 100 equiv of ethylbenzene (1.56×10^{-3} M) was mixed in CH_3CN (2.18 mL) in a quartz cell and cooled to -17 °C. Ferric perchlorate, $\text{Fe}(\text{ClO}_4)_3$, 25 equiv, (3.9×10^{-4} M) was mixed into the above solution. After a delay 0.5–1 s to permit formation of the porphyrin–iron(IV) diperchlorate species, the solution was irradiated with 20 pulses of light. The reaction mixture was warmed to room temperature and filtered through a short silica gel column. A known amount of internal standard was added to the filtrant for quantification, and the mixture was analyzed by GC and GC-mass spectrometry. The products, 1-phenylethanol and acetophenone, were identified by GC co-elution with authentic samples on both DB-5 and Carbowax columns and by mass spectral fragmentation patterns that were compared to those of the authentic samples. For the styrene and cyclooctene reactions, the products were identified as phenylacetaldehyde and cyclooctene oxide, respectively, by GC and GC-mass spectral analysis.

Acknowledgment. This work was supported by grants from the National Institutes of Health (GM48722) and the National Science Foundation (CHE-0601857).

JA807847Q

(43) Ha, C.; Horner, J. H.; Newcomb, M.; Varick, T. R.; Arnold, B. R.; Luszyk, J. *J. Org. Chem.* **1993**, *58*, 1194–1198.

(44) Johnson, C. C.; Horner, J. H.; Tronche, C.; Newcomb, M. *J. Am. Chem. Soc.* **1995**, *117*, 1684–1687.